

PROGRESS REPORT ON THE MILAN SUPERCONDUCTING CYCLOTRON

E. Acerbi, F. Aghion, F. Alessandria, G. Baccaglioni, G. Bellomo, C. Birattari, A. Bosotti, G. Cuttone\*, P. Di Bernardo\*, C. De Martinis, E. Fabrici, A. Ferrari, D. Giove, W. Giussani, S. Gustafsson\*, P. Michelato, C. Pagani, G. Raia\*, G. Rivoltella, L. Rossi, L. Serafini, A. Sussetto, V. Torri, G. Varisco  
 Università degli Studi di Milano - Istituto Nazionale di Fisica Nucleare Sezione di Milano  
 \* Laboratorio Nazionale del Sud di Catania

Summary

A  $K = 800$  superconducting cyclotron is under construction at the University of Milan. The machine will be tested with axially injected beams delivered by an ECR source before the installation at the Laboratorio Nazionale del Sud in Catania and the coupling to the 15 MV Tandem.

The status of the project, with a review of all the major machine components and a discussion of the difficulties encountered in their realization, is presented.

Introduction

A heavy ion facility, funded by Istituto Nazionale di Fisica Nucleare (INFN), is planned at the Laboratorio Nazionale del Sud (LNS) in Catania. The facility is based on an MP Tandem injecting radially into a booster K800 superconducting cyclotron. Two Laboratories collaborate for its realization: the Milan group takes care mainly of the design, construction and test of the compact superconducting cyclotron and the Catania group will provide for the coupling with the 15 MV Tandem, installed at LNS, and for the construction of the beam transfer lines to the experimental hall.

This accelerator complex will deliver ion beams of 100 MeV/n for light elements and 20 MeV/n for uranium (see Fig. 1). The beam intensities are expected to range from  $0.5 - 1 \cdot 10^{12}$  pps for light ions to  $0.5 - 1 \cdot 10^{11}$  pps for the heaviest ions. The extracted beams will have an energy spread of 0.1 - 0.2% with emittances of 6 - 10 mm mrad and a duty cycle of 2 - 3%.

The main characteristics of the Tandem and its improvements for the coupling with the cyclotron are reported elsewhere (1-3). The general features of the project and a detailed review of the superconducting cyclotron characteristics have been presented in several papers (4-17). Here, for the sake of completeness, we just recall the main parameters.

The three sector cyclotron (1.8 m pole diameter, 8.6 cm hill gap, 2.2 rad/m average spiral constant, 4.8 Tesla maximum average magnetic field) has a bending factor  $K = 800$  and a focusing factor  $K_f = 200$ . Three RF resonators, working in the frequency range 15 - 48 MHz, can accelerate the beams with the fundamental harmonic ( $h = 1$ ) or secondary harmonics ( $h = 2, 3$ ). The dee voltage is on average 100 kV and the installed power for each resonator is 90 kW.

Because detailed discussions on the various machine components are given elsewhere (18-28) at this Conference, this paper will present an overview of the project and the progress made so far in the construction of both the machine and the new laboratory.

General design

At the end of 85 it was decided to modify the initial program for the test of the machine, that foresaw the exploitation of an internal PIG source, and to re-

sort to an axial injection of the beam from an ECR source.

An axial injection system has been under study from the beginning of the project although planned for realization after the installation of the machine in Catania. The ECR source, similar to the LIS source now under construction at KFA Julich (29), will operate at voltages up to 20 kV with expected emittances in the range 150 - 300 mm mrad.

This compact and low cost source, delivering beams up to argon, will be used initially for the test of the machine and later for the acceleration of very light

ions ( $H_2^+$ , deuterons and alpha) not injectable from the Tandem into the cyclotron. A source with up to date performances and delivering also metallic ions can be added later in Catania in view of the promising development of the ECR source as indicated in Fig. 1.

The axial injection system has been designed to allow the installation of the ECR source in the cyclotron pit (18). In the Fig. 2 is shown a view of the ECR source and of the axial injection line placed at the bot-

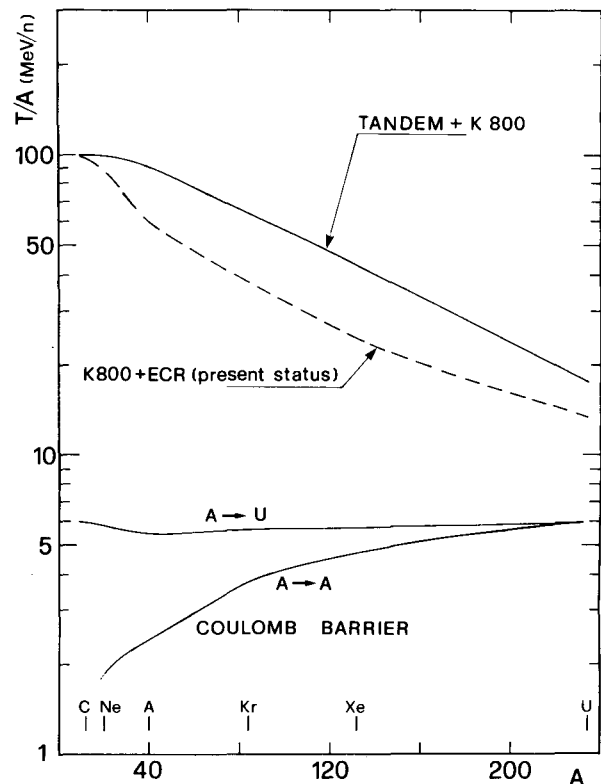


Fig. 1 Energy performances for the Tandem-cyclotron complex (full line) and for the cyclotron equipped with an ECR source (dashed line).

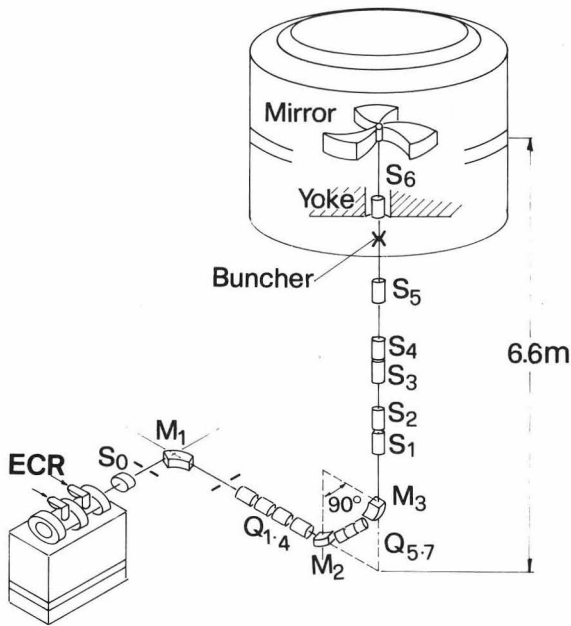


Fig. 2 Perspective view of the ECR source and axial injection system for the cyclotron.

tom of the cyclotron pit. A solenoid  $S_0$  refocuses the extracted beam at the entrance of the  $^o$ charge state analysing system. Four quadrupoles provide the independent matching in the two transversal planes. A  $90^\circ$  bending unit brings the beam on the cyclotron axis where a telescopic system (solenoids  $S_1 - S_4$ ) transports the beam up to 3 m from the median plane. The two solenoids  $S_5 - S_6$  keep the beam confined during the motion in the axial magnetic field of the cyclotron. An electrostatic mirror deflects the beam into the median plane: the mirror has an outer shell diameter  $\phi = 25$  mm and operates up to 17.5 kV.

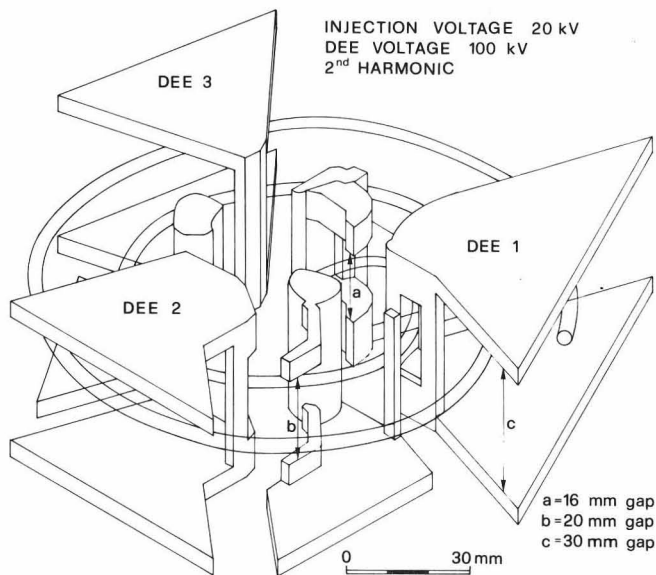


Fig. 3 Perspective view of the central region for operation in the  $h = 2$  harmonic mode.

A buncher will be installed close to the yoke hole entrance to improve the transmission.

The central region geometry has been optimized<sup>(19)</sup> for the  $h = 2$  harmonic mode because it allows to accelerate beams over the fully energy range of the machine (8 - 100 MeV/n). The possibility to operate in the  $h = 1$  harmonic mode has however been preserved. Acceptance of the central region, of the order of 500 mm mrad in both planes, matches well the emittance of the injected beam.

The configuration of the electrodes and the beam envelope are shown in the perspective view of Fig. 3.

A general study has been made to evaluate the effects of the dee-dee capacitive coupling in order to design a control system to assure stable operation of the cavities. A neutralising system has been devised, based on the recycling of the disturbing reactive power in a closed loop, which does not affect the operating characteristics of the RF cavities<sup>(20)</sup>. The study has also indicated that no neutralising system is needed if the coupling capacitances are lower than  $10^{-2}$  pF. Efforts have been made, successfully, in the design of the central region to limit the coupling capacitances below this value. Test with the three dee operation will be made to confirm the validity of the choice.

The design of the coupling line between the Tandem and the cyclotron has been completed<sup>(28)</sup>. The beam transport line, about 40 m long, has been designed in modular way to simplify the set-up and the tuning and to provide a decoupling between the two machines.

A two stage bunching system will produce at the cyclotron stripper a pulsed beam with a length of 3 RF degrees.

#### Project status

In the following a general description of the machine components, with the emphasis on test procedures, measuring apparatus and plants, is presented.

As a general remark on the status we recall that the project has met technical difficulties concerning the weldings of the LHe vessel and the performances of the ceramic insulator for the RF resonator. The building construction has undergone a large delay preventing the installation of the general and cryogenic plants up to beginning of this year. These delays have heavily affected the time schedule of the project.

#### Magnet.

The magnet yoke has been completed and installed in the new laboratory as shown in Fig. 4. The magnet pole cap is visible in foreground and the structure for the assembly of the cryostat in background.

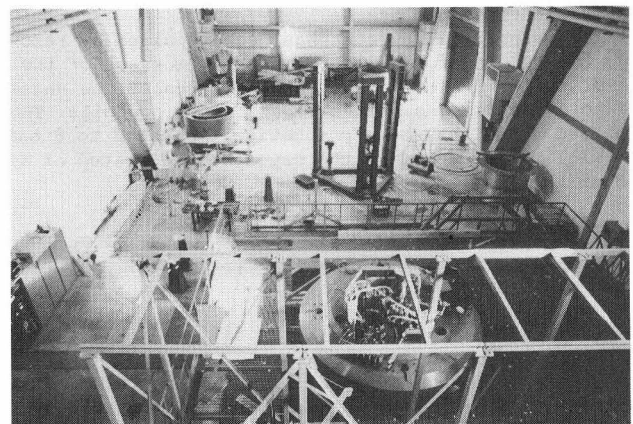


Fig. 4 View of the cyclotron hall



The trim coils, epoxy impregnated, have been assembled on the hill sectors (Fig. 5) and completed with the electric and water connections (Fig. 6).

Also the trim coil power supplies (500 A - 36 V and 400 A - 48 V) have been tested and installed in the new laboratory.

The power supplies of the main coils ( $I = 2000$  A,  $V = 20$  V, stability and reproducibility  $\pm 20$  mA) have been tested on a resistor load ( $R = 0.01 \Omega$ ) at full power and on a magnet ( $L = 0.2$  H) at low current.

The protection circuit for the superconducting coils has been tested using an AC supply ( $I_{\text{eff}} = 2000$  A) and discharging in the dump resistors 52 MJ in 25 s (the stored energy of the magnet is about 40 MJ). The maximum temperature measured in the resistors was 220 C (their limiting temperature is 400 C) and the cooling down to room temperature by forced air convection required half an hour.

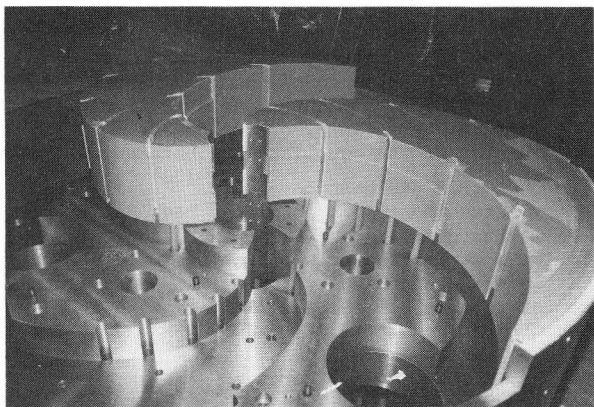


Fig. 5 Trim coils assembled on the hill sectors.

#### Cryostat.

The helium vessel has undergone the repair of four circumferential weldings which were not in conformity with the design specifications. The Charpy impact test values of the weldings at LHe temperature were lower than the required ones and the ferrite content was too high.

Several analysis on the welding samples (magnetic permeability measurements, chemical analysis, metallographic test, surface analysis with electron scanning and Auger microscopes) indicate that the defect was produced by the bare electrodes used in the last welding passes. These electrodes were from a different heat respect to the ones used in the qualification test and in the first two passes.

Therefore the cryostat has been repaired by removing the welding for about 8 mm (the thickness of the vessel is 10 mm) to keep hermetically sealed the vessel and to avoid damages to the superconducting coils. The repaired vessel has been pneumatically tested to 8 bar and will be assembled in the cryostat and tested at the end of this year.

#### Cryogenic plant.

The Fig. 7 shows a scheme of the cryogenic plant which consists of three sections:

- He liquifier and refrigerator
- He gas recovery and stockage
- LN stockage and distribution.

The refrigerator and liquifier system (TCF 100 - Sulzer), supplied by a two stage compressor delivers 80 W refrigeration power or 30 l/h of LHe (without LN precooling) and 120 W or 45 l/h (with LN precooling). It is equipped with two ejectors, respectively at room temperature and at He return vapour temperature, which

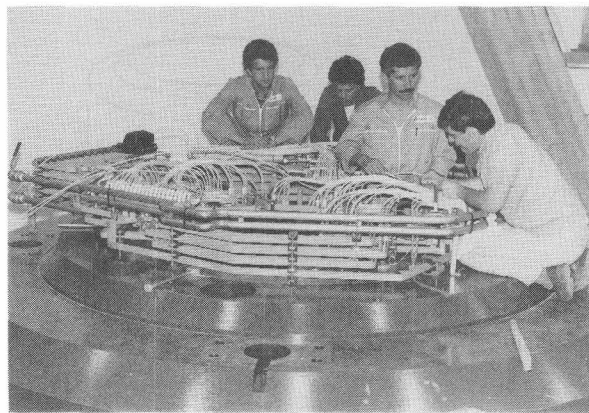


Fig. 6 Electrical and water connections of the trim coils.

make the operating pressure in the cryostat independent by the suction pressure of the compressor.

The recovery system consists of a balloon (volume  $10 \text{ m}^3$ , maximum overpressure 60 mbar), a four stage compressor with a two speed motor, a purifier (AR 14/200 - Linde) suitable to treat, without filter regeneration, about  $800 \text{ m}^3$  of helium with an impurity content of 0.5% and four vessels (capacity 7200 l) for the He gas stockage at 220 bar.

The LN is stored in a  $10^4$  l tank and is distributed at low pressure to the cryostat (about 10 l/h for the thermal shield), to the liquefier (25 - 30 l/h only if the precooling is exploited), to the purifier and to the TL1 - TL2 transfer lines (2 - 3 l/h).

During the normal operation the liquifier supplies a 1000 l dewar (line TL3) which compensates the fluctuations in the LHe production and consumption and assures during a liquifier failure, at least, 36 hours of operation.

From the dewar the LHe passes through a regulation valve in the cryostat; the cold vapours produced by expansion and thermal losses return to the refrigerator along TL1 and TL3 sucked by the cold ejector. The gas used to cool the current leads returns to the compressor through the warm ejector.

The pressure in the cryostat in normal operation is 1.05 - 1.10 bar and it can be controlled by a back pressure regulator installed on the return section of the TL1 line. The cryostat has been designed for a maximum pressure of 6.3 bar. If the pressure in the LHe vessel increases (quench or vacuum failure) a safety valve is opened at 4.4 bar. In any case a 4" bursting disk calibrated to 5.7 bar assures the vessel safety. The rationale of the high pressures in the safety valve and disk is that during the cool down working pressures of about 4 bar are required.

The expelled gases, when the safety valve is opened, are not recovered and are removed outside the laboratory. During the cool down the cryostat is supplied directly by the cold box through the TL1 line.

In the case of liquifier failure the evaporated gas can be fully recovered in the high pressure cylinders. At the beginning the recovery compressor works discontinuously removing the gas from the balloon and filling the first cylinder without purification. Later on, when also the purifier is running, the recovery compressor works continuously because it is supplied by the evaporated gas and by the stored gas of the first cylinder.

#### Magnetic field mapping system.

The magnetic field will be measured by flip coils, each connected to its own integrator. The flip coil has approximately 680 turns of copper wire (0.09 mm in diameter) wound on a MACOR bobbin. Its dimensions (I.D.



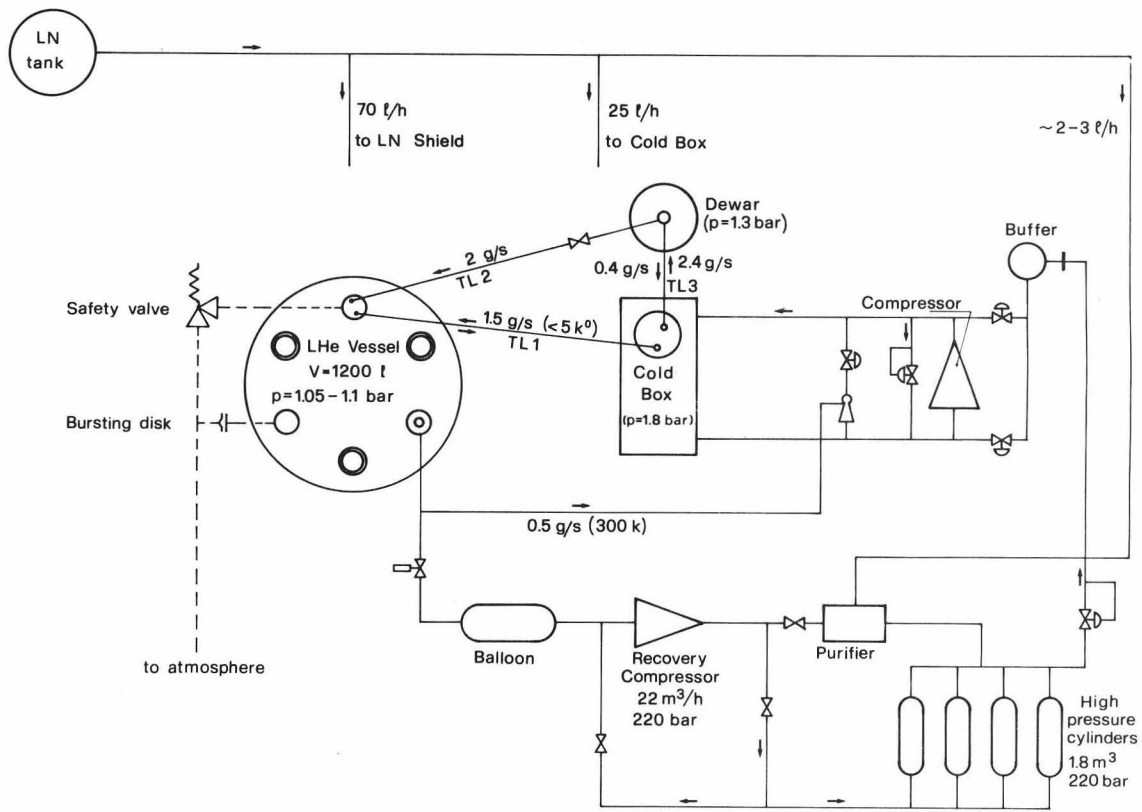


Fig. 7 Operational scheme of the cryogenic plant consisting of the LHe liquifier, He purifier and LN distribution.

4.3 mm, O.D. 7.6 mm and height 5.0 mm minimize the measuring errors arising by the cyclotron field gradient. The main components of the integrator circuit are: the AD 235K chopper stabilized amplifier (open loop gain  $> 5 \cdot 10^7$  V/V, input voltage drift  $\bar{+} 0.25$  V/C), the 0.5  $\mu$ F polystyrene capacitor (temperature coefficient - 120 ppm/C, insulation resistance  $10^{12} \Omega$  and low dielectric absorption) and the 40 K  $\Omega$  wirewound resistor (temperature coefficient + 2 ppm/C). All integration circuits are thermostabilized at 37 C (temperature stability 0.1 C): in these conditions the maximum measured drift is typically 100  $\mu$ V/s.

The drift and the temperature are measured each time before to flip the coil and the measured voltages are corrected by the drift and normalized to a reference temperature of 25 C. The average sensitivity of the flip coils is 1.8 V/T.

The magnetic field measuring system consists of four positioning elements: the calibration, the polar field, the axial field and the fringing field apparatus. Since the flip coil calibration and magnetic field measurement in the polar region require high accuracy (respectively  $\bar{+} 0.5 \cdot 10^{-4}$  and  $\bar{+} 1 \cdot 10^{-4}$ ) a particular care has been posed in the corresponding devices.

The calibration apparatus (Fig. 8) consists of a magnet (6 cm gap - 42 cm pole diameter) with an high stability power supply ( $1 \cdot 10^{-5}$ ) where the flip coils are calibrated in magnetic fields up to 1.45 T against a NMR probe. First the magnetic field is measured in several points along the H magnet centerline by the NMR probe, then the NMR probe is positioned near the pole edge (suitably shimmed) to control the field stability during the flip coil calibration. The homogeneity of the field along the magnet centerline allows the simultaneous calibration of 6 flip coils.

In the polar field apparatus (see scheme in Fig.9) 92 flip coils, mounted on a perspex rod and radially spaced of 10 mm, can be rotated through  $180^\circ$  by a pneumatic valve and conic gear. The rod support in fiber-glass G11 can be positioned azimuthally each  $2^\circ$  with an accuracy of 0.01°. This accuracy is obtained by means of a toothed-wheel (1.8 m in diameter) already used in 1963 for the magnetic field measurements of the Milan AVF cyclotron.

The flip coils rod can be centered mechanically to 0.05 mm with respect to the poles and the rotating arm (see Fig. 9) can be assembled in two opposite positions to check by means of magnetic measurements the construction or positioning errors in the toothed-wheel which

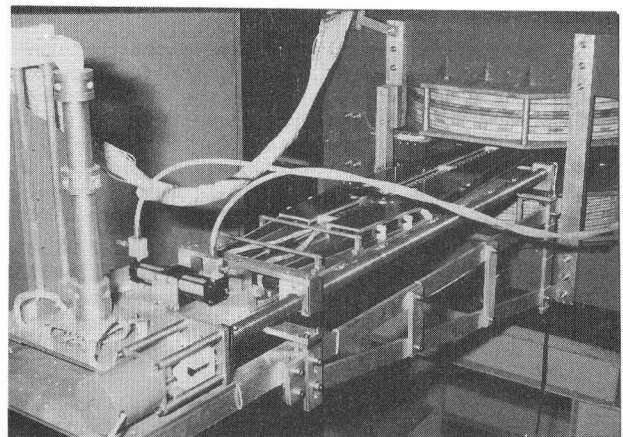


Fig. 8 Apparatus for the flip coil calibration.



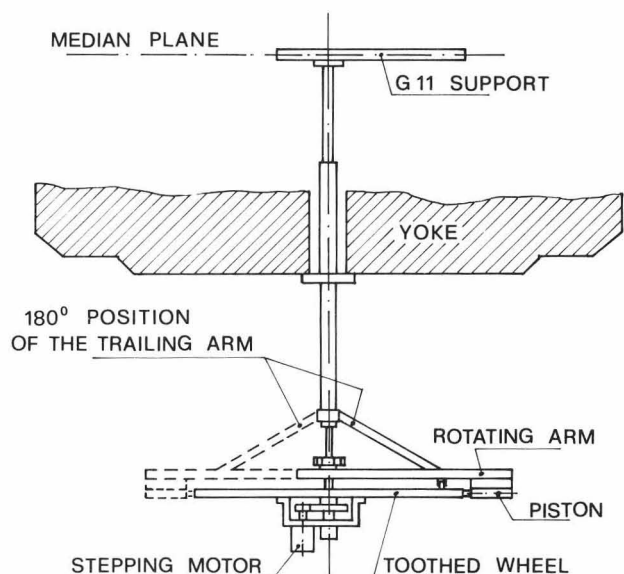


Fig. 9 Scheme of the apparatus for the polar field mapping.

could introduce spurious first harmonic components in the measured field.

RF system.

Full power tests. The full power tests on the first upper half cavity were successfully completed in spring 1986, after the change of the previous type of ceramic insulator, which was of very poor quality (Q factor 50 time lower than the guaranteed one).

The results (21,22) have shown that all the major components (ceramic insulator, sliding short, coupling capacitor) and design criteria are adequate and can be used for the final accelerating system. Nevertheless some minor modifications have been decided before to start the cavities fabrication, mainly to simplify the assembling procedure. We expect to receive the three final cavities by the end of this year.

During these tests, a prototype of the control electronics, for a simple and safe cavity operation, was used together with amplitude and phase feedback loops. Since they behaved according to the project goals we are now redesigning the RF control system, based on these circuits, but computer controlled.

Computing. A complete analysis of the cavity behaviour, mainly in the ceramic insulator region, has been performed (23) using an implemented version of the computer code SUPERFISH. As a result, a small modification of this region was decided to increase the maximum operating frequency from the measured 47 MHz to 49.5 MHz. This change, which mainly consists in few volume displacements leaving the insulator in the same position, slightly reduces the electric field in some critical points, like for example the inner coaxial corona ring.

Power amplifiers. The three BBC RF power amplifiers have been installed into the new cyclotron building and they are now under test on dummy load, to optimize their already good performances. The 6 1/8" feeders for connection to the cavity resonators will be installed in the near future.

Liner. A conceptual design of the liner has been done and the main decisions on the technology that will be used have been taken. Also a complete set of measurements of the effective geometry of the magnet hills,

with all the impregnated trim coils assembled, was carried out to verify the needed tolerances. We will mainly use milling machined copper sheets, 15 mm in thickness, for hills and valleys covers, TIG welded to lateral 3 mm sheets.

Also if we are anticipating the welding tests and the fabrication of some linear part or model, we have to wait at least the eventual correction of the valley deep, dictated by the magnetic measurements, to start the fabrication according to the final design.

Computer control.

A distributed architecture of powerful microprocessor based units, connected by an optical network with a star topology, has been designed (25) to perform the control of the machine.

The main elements of the network are a passive optical star coupler with a typical insertion loss of 0.5 dB, able to connect up to sixteen nodes together, and the communication devices providing optical transmit/receive capabilities (Codenoll Technology Corp.). Connection among the units is performed by means of two cords assembly, graded index optical fibers (100 μm core, 140 μm cladding).

In house tests have demonstrated a good reliability of the hardware; a bit error rate, between any two nodes, better than  $1 \cdot 10^{-9}$  has been measured.

Each node of the network has been designed using a standard card-cage equipped with a microcomputer for communication control and at least one CPU board both based on sixteen bits microprocessors with 0.5 Megabytes of memory.

Following the needs of each application the standard control station has been customized using specialized I/O modules for digital control, analogue data acquisition and close-loop control.

The software structure has been organized in such a way that first level processing of signals is performed by the I/O modules themselves. The CPU boards in which a nucleus of an operating system has been implemented (iRMX86), perform the real-time control of the equipment connected to the I/O modules, execute tasks activated by commands issued by the console or the host computer, and convert data to physics units.

The console (24), a prototype is shown in Fig. 10, uses dedicated boards for driving color and B/W gra-



Fig. 10 Prototype of the control console.



phic monitors, touch panels and other interactive devices.

The host computer (DEC microVAX II) up to now has the function to maintain a centralized database, to check the network and the peripheral control stations and to perform the start-up of the control system. In future it will determine the right operational configuration of the cyclotron parameters for each ion selected for acceleration and for each experimental set-up.

#### Axial injection.

The components of the ECR source have been ordered, and their assembly will start at the end of this year.

All elements of the beam line are under construction with the exception of the solenoids  $S_5$  and  $S_6$  whose parameters will be defined after the mapping of the axial field of the cyclotron.

A prototype of the electrostatic mirror is under development.

It is planned to test part of the beam line with the beam delivered by the ECR source before its final installation into the cyclotron pit.

#### Extraction.

The extraction design has been completely defined and no change have been made.

Work on the high voltage deflector is in progress<sup>(26)</sup>. A new test stand with a stainless steel vacuum chamber and a 10 kGauss magnet has been installed in order to investigate the behaviour of the electrical discharge in the presence of the magnetic field which has a strong influence on the voltage hold off capability. A new 150 kV - 3 mA power supply has been delivered by the firm Heinzinger, with a current limit and an automatic recovery after a discharge which has proved to be useful in reducing the time for conditioning and testing.

Extensive tests have been carried out on a full scale prototype of the deflector with the length reduced to 1/3 of the nominal value, in order to select the best combination of electrode and liner materials. AISI 304 stainless steel and titanium have been checked as high voltage electrode and molybdenum, tungsten and tantalum for the liners. The optimal combination seems to be titanium with tungsten.

Preliminary results in the 10 kGauss magnet look promising: electric field in the gap of the order of 120 kV/cm have been sustained for long time with a few discharges per hour.

Moreover a new electrode geometry has been investigated with POISSON calculations: the aim being to reduce the electrical field strength mainly in the region where it is parallel to the magnetic field lines. Best results have been obtained with an electrode configuration with different radii of curvature. The highest calculated electric field is of the order of 157 kV/cm for 100 kV voltage, a value which is a 15% lower than the edges rounded with a constant radius of 5 mm.

#### Vacuum.

The cyclotron has three separated vacuum systems respectively for the acceleration chamber (residual pressure  $1-2 \cdot 10^{-7}$  torr), the liner-pole region (coarse vacuum  $<1$  torr) and the cryostat (residual pressure  $0.5-1 \cdot 10^{-5}$  torr). The liner pole region is pumped through 6 tubes (30 mm in diameter, 1.5 m long) by two rotary pumps (each  $30 \text{ m}^3/\text{h}$ ). The cryostat chamber is pumped from the bottom flange by two diffusion pumps (effective pumping speed 400 l/s).

To obtain in the acceleration region the required pressure some special techniques have been adopted<sup>(27)</sup>. The use of splitted refrigerator cooled cryopump instal-

led in the dees and the nickel plating of the iron walls of the vacuum chamber (Fig. 11) should assure the required vacuum. The cryopump prototype, made by Leybold Heraeus has been successfully tested in our laboratory. The pump worked continuously for about 1000 hours without any trouble and the pumping characteristics are acceptable. Tests have been carried out in the magnetic field of the Milan AVF cyclotron to control the mechanical and thermal behaviour of the pump. These tests showed that the pump is able to work in worst conditions then those met in the K800 magnet. So it was decided to use 3 splitted pumps, with some improvements (easier assembling operations and larger cooling power) respect to the prototype, for the high vacuum pumping system of the cyclotron.

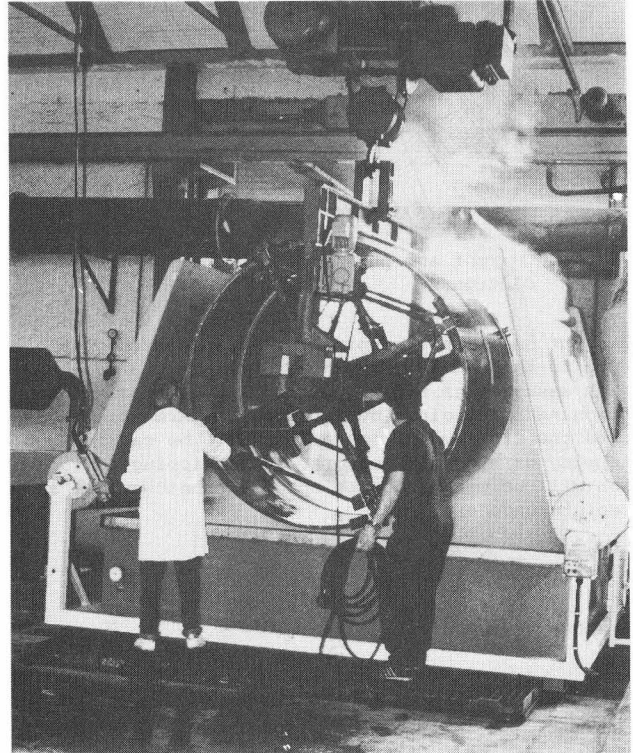


Fig. 11 Internal vacuum chamber wall during the nickel plating operations.

#### Diagnostic.

The main diagnostic devices for the internal beam will be:

- a current probe suitable for integral and differential measurements with three or five fingers (water cooled) and moving along an hill centerline from 15 cm radius up to extraction radius;
- two extraction probes (differential probes with a short range  $\sim 1$  cm) to control the position and the size of the beam in front of the electrostatic deflectors.

The possibility to place current probes, in the two other hills, at two given radii for beam centering is under investigation.

Ten phase probes, equally spaced radially, and located on the hill centerline, are planned for the control of the isochronism. The characteristics of these phase probes are under study in order to optimize their performances for all the accelerated beams.

The probe location and the region occupied by the stripping foil are shown in Fig. 12.

A preliminary design of the stripper apparatus has been carried out (Fig. 13). At the top of the cyclotron there is a vacuum sealed reservoir of stripping foils from which a tape takes away new foil by unloading the



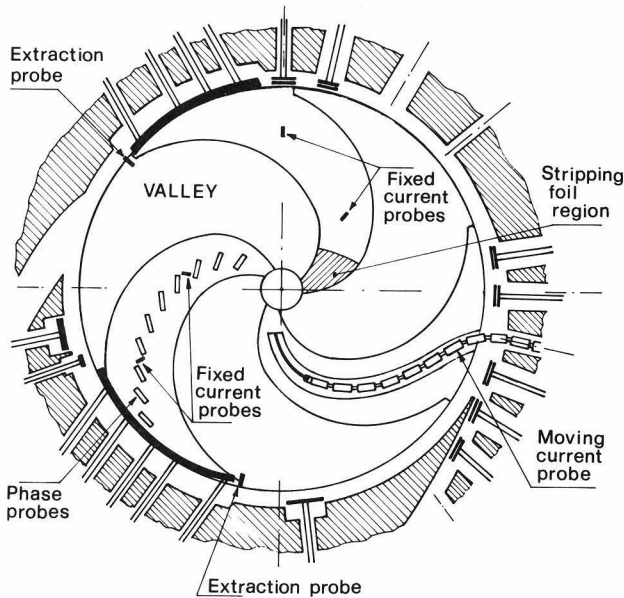


Fig. 12 Current and phase probes location in the cyclotron.

worn out one. The stripping foil transported by the tape up to the median plane is installed in a trolley which assures its radial positioning. The azimuthal positioning is obtained by rotating the arm which supports the trolley. All movements will be carried out by stepping or hydraulic motors. The stripping foil position will be measured with optoelectronic system and absolute encoders.

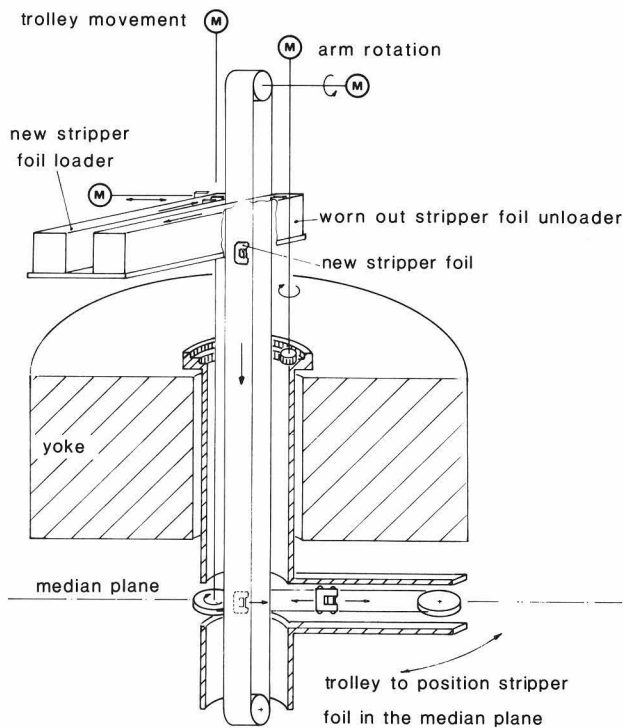


Fig. 13 Scheme of the stripping foil apparatus.

Health physics.

For the beam tests a complete radioprotective apparatus (shields, interlocks, monitors etc.) must be realised. An evaluation of the intensity of the radiation levels has been carried out and the main characteristics of the radioprotection system defined. Since the beam tests will go on in Milan only for a limited time, a temporary concrete shield will be employed in order to reduce the neutron fluence.

Due to the large stripping cross section, the deuterons are, among the ions which will be accelerated, the worst possible case for the neutron yield, the neutron energy and angular distribution. Therefore in order to evaluate the characteristics of the radioprotection system and the shielding thickness, the spectra and angular distribution of neutrons produced by deuterons impinging on a thick carbon target have been examined. Neutron spectra have been calculated following the models of Serber and Nakamura (30,31) for the relative contributions of the stripping, preequilibrium, equilibrium and slowing down processes. The calculations give a total yield of 0.7 neutron for incident deuteron. The spectra computed at different emission angles are presented in Fig. 14.

The planned beam tests will cover no more than 2000 hours over one year. Limits for the total equivalent dose of 15 mSv for the occupationally exposed workers and of 1 mSv for the members of the public have been assumed. Since the accelerator is partially self-shielding and given an average intensity of the deuteron beam of  $10^{11}$  pps, a 2 m thick ordinary concrete shield around the accelerator is required. If the lateral shield walls are high enough (typically about 6m), no shielding of the roof is required.

Airborne radioactivity induced by neutrons has also been evaluated giving a concentration of radionuclides produced in the air not as high as to require a forced ventilation of the cyclotron vault.

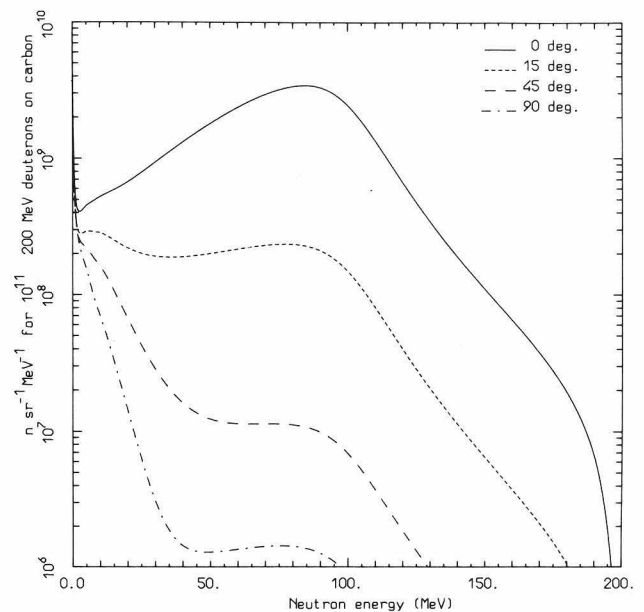


Fig. 14 Computed spectra of neutrons emitted at various angles by a carbon target with 200 MeV incident deuterons

Building status

The new building for the cyclotron (hangar, power supply rooms, technical plant room, workshop, control room etc) for about 3500 m<sup>2</sup> of area and about 20000 m<sup>3</sup>

of volume began to be available for the installation of general plants (electric power, heating and air conditioning system etc.) and special plants (power and RF supply, cryogenic system, water cooling system etc) in September 1985.

These systems are now completed (except the cryogenic plant) and in operation.

Offices and laboratories for about 2500 m<sup>2</sup> of area are planned to be completed for the end of the year.

The delay was caused mainly by discontinuity in the funding. Therefore the whole complex will be operational in spring 87.

The building, as in September 1986, is shown in Fig. 15.

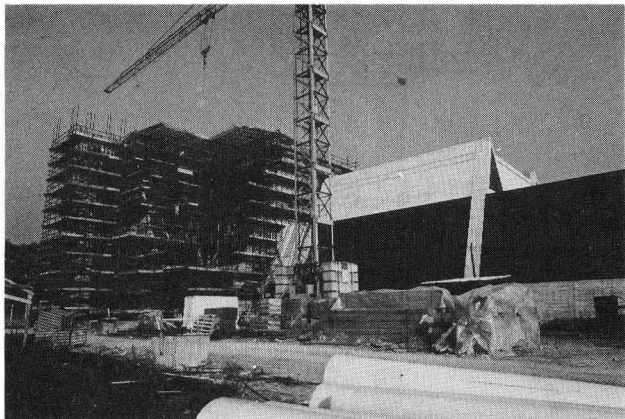


Fig. 15 View of the new laboratory buildings

#### Conclusions

As discussed before the time required to carry out the tests on the welding samples and the LHe vessel repair and the impossibility to dispose of the building before the end of 1985 are the major causes of the delay undergone by the project.

The construction of the cyclotron will proceed vigorously from the beginning of the next year, with the tests of the magnet (cool down, coils excitation, magnetic field measurements).

The first extracted beam is expected for the end of 1988 and the installation at LNS in Catania during the 1989.

#### References

- 1) E. Migneco, NIM 220, (1984) 14
- 2) L. Calabretta et al., NIM 220, (1984) 158
- 3) G. Ciavola et al., NIM 244, (1984) 162
- 4-9) E. Acerbi et al., Proc. 9<sup>th</sup> Conf. on Cyclotrons and their Appl. (Caen - 1981) Les Editions de Physique. Pages: 169, 395, 399, 423, 501, 613
- 10-17) E. Acerbi et al., Proc. 10<sup>th</sup> Conf. on Cyclotrons and their Appl. (East Lansing- 1984) IEEE catalog N. 84CH 1966-3
- 18) G. Bellomo, The axial injection project for the Milan superconducting cyclotron, this Conference
- 19) G. Bellomo et al., Design of the central region for axial injection in the Milan superconducting cyclotron, this Conference
- 20) S. Gustafsson et al., Effects and control of the dee to dee coupling capacitances, this Conference
- 21) A. Bosotti et al., Full power tests of the first RF cavity for the Milan K800 cyclotron, this Conference

- 22) C. Pagani, Very high performance sliding short for RF resonators tuning, this Conference
- 23) L. Serafini et al., Electromagnetic calculations for an improved design of the Milan K800 cyclotron RF cavities, this Conference
- 24) F. Agion et al., The operator interface in the control system for the Milan superconducting cyclotron, this Conference
- 25) F. Agion et al., The distributed control system with decentralized access to an optical bus for the Milan superconducting cyclotron, this Conference
- 26) C. De Martinis et al., High voltage experiments for the electrostatic deflector of the Milan superconducting cyclotron, this Conference
- 27) P. Michelato et al., The Milan K800 cyclotron vacuum system, this Conference
- 28) G. Bellomo et al., The coupling line between the Tandem and the superconducting cyclotron at the LNS in Catania, this Conference
- 29) H. Beuscher et al., KFA Julich IKP Annual Report 1984, page 328
- 30) R. Serber, Phys. Rev. 72 (1947) 1008
- 31) T. Nakamura et al., Phys. Rev. C29 (1984) 1317